

# Synthesis of Conjugated *bis*-Schiff Base and Their Complexes as Dye-Sensitizer for Dye Sensitized Solar Cell (DSSC) Application

NURSYAFIRA ADZIRA HALMI\* & MENG GUAN TAY

Faculty of Resource Science and Technology, Universiti Malaysia Sarawak, 94300 Kota Samarahan, Sarawak, Malaysia

\*Corresponding author: [nursyafiraadzira@gmail.com](mailto:nursyafiraadzira@gmail.com)

Received: 23 July 2022

Accepted: 23 November 2022

Published: 31 December 2022

## ABSTRACT

Schiff base and their metal complexes have been widely used as photovoltaic materials due to their excellent  $\pi$ -electron transfer properties along the molecule. A total of eleven conjugated symmetrical bis-Schiff base and their complexes with different  $\pi$ -spacers have been synthesized and spectroscopically characterized in order to investigate their conversion efficiency in dye-sensitizer solar cells (DSSC). All compounds were either substituted with hydroxy (-OH) or methoxy (-OMe) as the electron donor and difluoro boron (BF<sub>2</sub>) as the electron acceptor or without any substituent. All compounds were applied as dye-sensitizer in DSSC using titanium (IV) oxide (TiO<sub>2</sub>) coated on a fluoride doped tin oxide glass as the working electrode and electric paint containing carbon black, whereas graphene coated indium tin oxide glass as the counter electrode. The power conversion efficiencies of the eleven bis-Schiff bases were compared to N3 Dye as the benchmark standard. The results showed that the compound with aromatic ring bridge as the  $\pi$ -spacer and -OMe substituent gave the highest efficiency at 0.0691% whereas the compound with aromatic ring and BF<sub>2</sub> gave the lowest efficiency at 0.0012%.

**Keywords:** Conversion efficiency, dye-sensitized solar cells, dye-sensitizer, symmetrical bis-Schiff-base,  $\pi$ -conjugated system

Copyright: This is an open access article distributed under the terms of the CC-BY-NC-SA (Creative Commons Attribution-NonCommercial-ShareAlike 4.0 International License) which permits unrestricted use, distribution, and reproduction in any medium, for non-commercial purposes, provided the original work of the author(s) is properly cited.

## INTRODUCTION

In the current solar cell market, silicon-based cells are dominating with 90% of the commercialized solar cells due to their high efficiencies (Gul *et al.*, 2016; Milichko *et al.*, 2016; Shubbak, 2019). However, despite having high efficiencies, this technology is expensive due to the complicated fabrication technique (Pandey *et al.*, 2016). As the result, dye-sensitized solar cells (DSSC) were developed which offered low cost as well as easy preparation. Although DSSC technology has yet to be commercially proven due to its low efficiencies compared to silicon type solar cells, DSSC is highly promising which attracts many researchers to continue extensive research to improve this technology (Nain & Kumar, 2021). Among all the components of DSSC, dye-sensitizer plays a vital role in improving the efficiency in DSSC as it acts as the solar harvester to convert solar energy into electrical energy (Alhamed *et al.*, 2012). By understanding the relationship between chemical structures and

their function in the devices, chemists can design the dyes to enhance their efficiency of the dyes.

Schiff base and their metal complexes have been used widely as photovoltaic materials as they have the potential photovoltaic characteristics (Teo *et al.*, 2017; Phan *et al.*, 2019). Many soluble extended  $\pi$ -conjugated materials based on Schiff base metal complexes have been studied as sensitizers for wide-bandgap oxide semiconductors such as TiO<sub>2</sub> and showed a good degree of conversion efficiency (Mahadevi & Sumathi, 2020). According to Lokhande *et al.* (2019), the reasons Schiff bases can be utilized as dye-sensitizer for DSSC is that they can absorb visible radiation and undergo charge transitions. In fact, substantial research has shown that the metal complexation of Schiff bases (Tay *et al.*, 2013) has a significant impact on their activity as well as their optoelectronic properties. As a result, they could be used as sensitizers and acceptors in DSSC (Chouk *et al.*, 2019).

Herein, we report the power conversion efficiency (PCE) of eleven symmetrical bis-Schiff base compounds and complexes (Figure 1). The symmetrical bis-Schiff base compounds were synthesized in four different series with a

different  $\pi$ -spacer bridge. Substituents such as hydroxy (-OH) and methoxy (-OMe) were used as electron donors meanwhile difluoro boron ( $\text{BF}_2$ ) was used as electron acceptor.

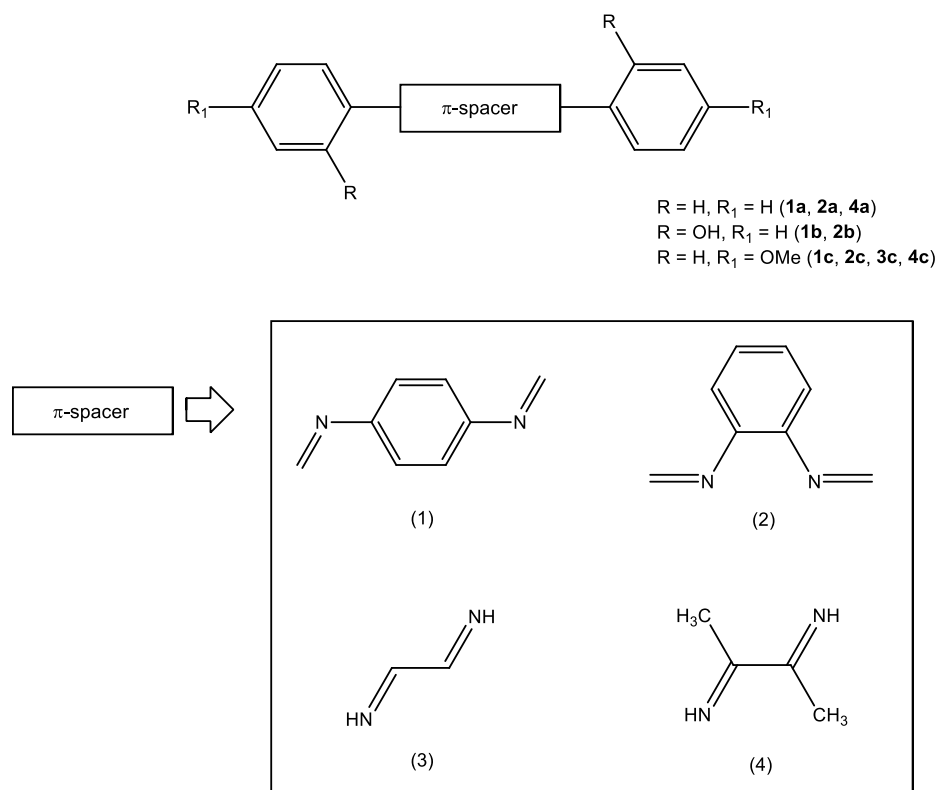


**Figure 1.** Four series of symmetrical bis-Schiff base derivatives with different  $\pi$ -spacer and substituents

By comparing compounds from series 1 (**1a**, **1b**, **1c** and **1d**) and series 2 (**2a**, **2b**, **2c** and **2d**), the effect of substituents can be observed through the PCE values whereas the effect of the different  $\pi$ -spacer bridges at the centre of the structure can be observed by comparing compounds **1c**, **2c**, **3c** and **4c**.

## METHODOLOGY

### Materials and Reagents

Chemicals namely *p*-phenylenediamine (MERCK), *o*-phenylenediamine (Fluka Chemica), glyoxal (MERCK), diacetyl (MERCK), 2-hydroxybenzaldehyde (MERCK), benzaldehyde (Bendosen), *p*-tolualdehyde (ALDRICH), *p*-anisaldehyde (ALDRICH), methyl-4-formylbenzoate (MERCK), aniline (R&M Chemicals), 2-aminophenol (MERCK), *p*-toluidine (MERCK), *p*-anisidine (MERCK), methyl-4-aminobenzoate (ALDRICH), boron trifluoride diethyl ether (MERCK),

triethylamine (MERCK), polyethylene glycol (ALDRICH), polyethylene glycol 20000 (MERCK), titanium (IV) oxide anatase (ALDRICH), potassium iodide (MERCK), iodine resublimed (R&M Chemicals), *cis*-Bis(isothiocyanato)bis(2,2'-bipyridyl-4,4' dicarboxylato) ruthenium(II), N3, dye (ALDRICH) and triton X-100 (ACROS Organics) were used as received without further purification otherwise stated.

Ethanol was purified by refluxing 900 ml of ethanol with 3.5 g of magnesium granular and 1.5 g of iodine until the solution turned colorless. Then the purified ethanol was collected *via* distillation.

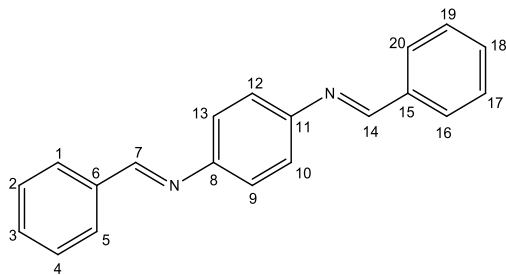
### Characterisations

The Fourier-transform infra-red (FT-IR) was conducted by using Thermo Scientific Nicolet iS10 FTIR spectrophotometer in KBr disc at the wavelength of 400 – 4000  $\text{cm}^{-1}$ . The  $^1\text{H}$  and  $^{13}\text{C}$

NMR spectra were obtained by using JEOL ECA-500 MHz NMR spectrophotometer with appropriate deuterated solvent ( $\text{CDCl}_3$ ; 7.26 ppm,  $\text{DMSO-d}_6$ :  $\delta\text{H}$  2.50 ppm) at room temperature and tetramethylsilane was used as the internal standard reference. The molecular weights of the compounds were recorded using Agilent 5977 GC/MS, under the following operating conditions: injector temperature at 280 °C, detector temperature 280 °C, the oven temperature increased at the rate 10 °C/min from 50 – 280 °C. Helium gas was used as the carrier gas. The percentage of carbon, hydrogen and nitrogen were recorded by using Thermo Scientific FlashSmart CHNS Analyzer. Lastly, the UV-Vis spectra were carried out using Agilent Cary 60 UV-Vis spectrophotometer with a 1 cm quartz cuvette in the range of 200 – 800 nm.

### Preparation of Symmetrical bis-Schiff Base Compounds

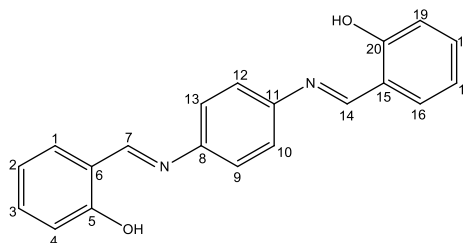
#### Preparation of ( $N^1E, N^4E$ )- $N^1, N^4$ -dibenzylidene benzene-1,4-diamine, (**1a**)



Benzaldehyde (10 mmol, 1.061 g) in 20 ml ethanol was added into *p*-phenylenediamine (5 mmol, 0.541 g) and refluxed while stirred for 2 hours at 80 °C. The precipitate formed was then filtered and washed a few times with 15 ml cold ethanol each time. The yellow precipitate was purified *via* slow diffusion of hexane into dichloromethane solution of the product. Yield: 1.391 g, 98%. IR (KBr,  $\text{cm}^{-1}$ )  $\nu$ : 3055.11 (C-H aromatic), 2884.38 (C-H vibration), 1615.70 (C=N stretching), 1574.49, 1492.07 (C=C aromatic), 1362.55 (C-N stretching).  $^1\text{H}$  NMR (500 MHz,  $\text{DMSO-d}_6$ ,  $\delta$  ppm) H: 8.69 (s, 2H, HC=N, H-7, 14), 7.96 (d, 4H,  $J$  = 9 Hz,  $\text{H}_{\text{aromatic}}$ , H-1, 5, 16, 20), 7.53 (m, 6H,  $\text{H}_{\text{aromatic}}$ , H-2, 3, 4, 17, 18, 19), 7.37 (s, 4H,  $\text{H}_{\text{aromatic}}$ , H-9, 10, 12, 13).  $^{13}\text{C}$  NMR (125 MHz,  $\text{DMSO-d}_6$ ,  $\delta$  ppm) C: 160.62 (C-7, 14), 149.99 (C-8, 11), 136.61 (C-6, 15), 131.90 (C-3, 18), 129.30 (C-1, 5, 20, 16), 129.11 (C-2, 4, 17, 19), 122.44 (C-9, 10, 12, 13).

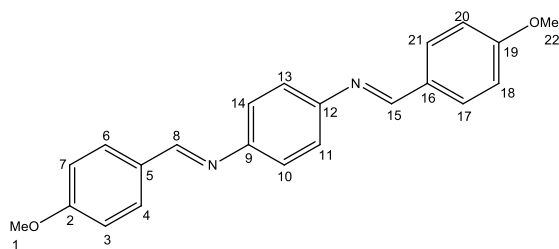
UV-Vis (DCM) ( $\lambda_{\text{max}}$ /nm): 273 and 355. Anal. Calcd. For  $\text{C}_{20}\text{H}_{16}\text{N}_2$ : C, 84.48; H, 5.67; N, 9.85. Found: C, 84.43; H, 5.53; N, 9.62. MS ( $m/z$ ): 284  $[\text{M}]^+$ .

#### Preparation of 2,2'-[(1E,1'E)-(1,4-phenylenebis(azanylylidene))bis(methanylylidene)]diphenol, (**1b**)



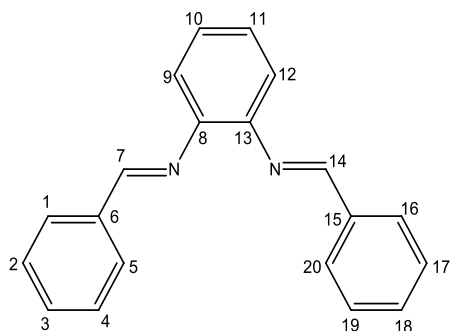
2-hydroxybenzaldehyde (10 mmol, 1.22 g) in 20 ml ethanol was added into 20 ml ethanolic solution of *p*-phenylenediamine (5 mmol, 0.541 g). The mixture then refluxed while stirred for 1 hour. Brown precipitate formed was then filtered and wash a few times using cold ethanol. Bright orange crystal was obtained *via* slow diffusion of hexane into dichloromethane solution of the powder. Yield: 1.493 g, 95%. IR (KBr,  $\text{cm}^{-1}$ )  $\nu$ : 3375.55 (OH), 2983.82 (C-H aromatic), 2868.77 (C-H vibration), 1600.45 (C=N stretching), 1567.58, 1485.40 (C=C aromatic), 1364.86 (C-N stretching), 1268.99 (C-O stretching).  $^1\text{H}$  NMR (500 MHz,  $\text{DMSO-d}_6$ ,  $\delta$  ppm) H: 9.03 (s, 2H, HC=N, H-7, 14), 7.68 (d, 2H,  $J$  = 7 Hz,  $\text{H}_{\text{aromatic}}$ , H-1, 16), 7.55 (s, 4H,  $\text{H}_{\text{aromatic}}$ , H-9, 10, 12, 13), 7.43 (t, 2H,  $J$  = 8 Hz,  $\text{H}_{\text{aromatic}}$ , H-3, 18), 6.99 (m, 4H,  $\text{H}_{\text{aromatic}}$ , H-2, 4, 17, 19).  $^{13}\text{C}$  NMR (125 MHz,  $\text{DMSO-d}_6$ ,  $\delta$  ppm) C: 163.74 (C-5, 20), 160.82 (C-7, 14), 147.15 (C-8, 11), 133.90 (C-3, 18), 133.00 (C-1, 16), 123.10 (C-9, 10, 12, 13), 119.90 (C-2, 17), 119.75 (C-6, 15), 117.06 (C-4, 19). UV-Vis (DCM) ( $\lambda_{\text{max}}$ /nm): 274 and 370. Anal. Calcd. For  $\text{C}_{20}\text{H}_{16}\text{N}_2\text{O}_2$ : C, 75.93; H, 5.10; N, 8.86. Found: C, 75.72; H, 4.95; N, 8.74. MS ( $m/z$ ): 316  $[\text{M}]^+$ .

#### Preparation of ( $N^1E, N^4E$ )- $N^1, N^4$ -bis(4-methoxybenzylidene)benzene-1,4-diamine, (**1c**)



The procedure was similar to **1a** but benzaldehyde was replaced with *p*-anisaldehyde (10 mmol, 1.362 g). The yellow precipitate formed was purified *via* recrystallization by using vapour diffusion of hexane into dichloromethane. Yield: 1.669 g, 97%. IR (KBr,  $\text{cm}^{-1}$ )  $\nu$ : 2955.03 (C-H aromatic), 2840.23 (C-H vibration), 1603.92 (C=N stretching), 1568.60, 1509.73 (C=C aromatic), 1300.74 (C-N stretching), 844.48 (*para*-Subst.).  $^1\text{H}$  NMR (500 MHz, DMSO- $d_6$ ,  $\delta$  ppm) H: 8.59 (s, 2H, HC=N, H-8, 15), 7.90 (d, 4H,  $J = 9$  Hz,  $H_{\text{aromatic}}$ , H-3, 7, 18, 20), 7.30 (s, 4H,  $H_{\text{aromatic}}$ , H-10, 11, 13, 14), 7.08 (d, 4H,  $J = 9$  Hz,  $H_{\text{aromatic}}$ , H-4, 6, 17, 21), 3.84 (s, 6H, H-1, 22).  $^{13}\text{C}$  NMR (125 MHz, DMSO- $d_6$ ,  $\delta$  ppm) C: 163.26 (C-2, 19), 160.00 (C-8, 15), 133.02 (C-9, 12), 131.54 (C-4, 6, 17, 21), 130.26 (C-5, 16), 122.77 (C-10, 11, 13, 14), 115.22 (C-3, 7, 18, 20), 56.45 (C-1, 22). UV-Vis (DCM) ( $\lambda_{\text{max}}/\text{nm}$ ): 297 and 367. Anal. Calcd. For  $\text{C}_{22}\text{H}_{20}\text{N}_2\text{O}_2$ : C, 76.72; H, 5.85; N, 8.13. Found: C, 76.84; H, 5.71; N, 7.74. MS ( $m/z$ ): 344  $[\text{M}]^+$ .

*Preparation of (N<sup>1</sup>E,N<sup>2</sup>E)-N<sup>1</sup>,N<sup>2</sup>-dibenzylidene benzene-1,2-diamine, (2a)*

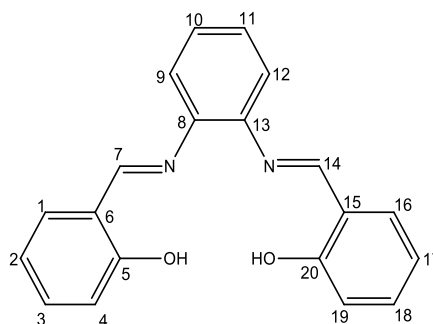


Ethanol solution of benzaldehyde (10 mmol, 1.061 g) was added into ethanol solution of *o*-phenylenediamine (5 mmol, 0.541 g). The mixture was refluxed for 8 hours at 80 °C. Then, the solvent was reduced until ~15 ml by using rotary evaporator. The dark concentrated mixture was left at room temperature until precipitate formed. The cream-coloured precipitate formed was then isolated and washed with cold ethanol a few times. Yield: 0.687 g,

54%. IR (KBr,  $\text{cm}^{-1}$ )  $\nu$ : 3057.78 (C-H aromatic), 2957.97 (C-H vibration), 1603.19 (C=N stretching), 1488.14, 1447.05 (C=C aromatic), 1392.26 (C-N stretching).  $^1\text{H}$  NMR (500 MHz, DMSO- $d_6$ ,  $\delta$  ppm) H: 7.88 (s, 1H, HC=N, H-7), 7.87 (s, 1H, HC=N, H-14), 7.69 (d, 2H,  $J = 7$  Hz,

$H_{\text{aromatic}}$ , H-1, 20), 7.45 (m, 4H,  $H_{\text{aromatic}}$ , H-9, 10, 11, 12), 7.26 (m, 6H,  $H_{\text{aromatic}}$ , H-2, 3, 4, 17, 18, 19), 7.09 (d, 2H,  $J = 7$  Hz,  $H_{\text{aromatic}}$ , H-5, 16).  $^{13}\text{C}$  NMR (125 MHz,  $\text{CDCl}_3$ ,  $\delta$  ppm) C: 154.16 (C-7), 142.88 (C-14), 136.40 (C-8), 136.06 (C-13), 130.17 (C-12), 129.91 (C-6, 15), 129.41 (C-1, 16), 129.21 (C-2, 17), 128.93 (C-5, 20), 127.66 (C-9), 126.09 (C-4, 19), 123.31 (C-3), 122.98 (C-18), 119.99 (C-10), 110.72 (C-11). UV-Vis (DCM) ( $\lambda_{\text{max}}/\text{nm}$ ): 292. Anal. Calcd. For  $\text{C}_{20}\text{H}_{16}\text{N}_2$ : C, 84.48; H, 5.67; N, 9.85. Found: C, 84.03; H, 5.67; N, 10.08. MS ( $m/z$ ): 284  $[\text{M}]^+$ .

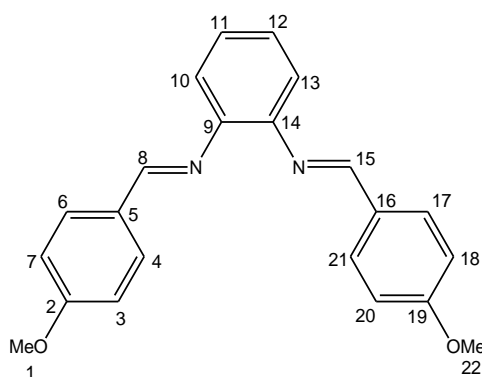
*Preparation of 2,2'-[(1E,1'E)-(1,2-phenylenebis (azanylylidene))bis(methanylylidene)]diphenol, (2b)*



The procedure was similar to **1b** but *p*-phenylenediamine was replaced by *o*-phenylenediamine (5 mmol, 0.541 g). The orange crystal was obtained *via* slow evaporation of the precipitate in chloroform:ethanol (10:1) mixture of solvent. Yield: 1.455 g, 92%. IR (KBr,  $\text{cm}^{-1}$ )  $\nu$ : 3320.03 (OH), 2925.59 (C-H aromatic), 2887.33 (C-H vibration), 1606.87 (C=N stretching), 1556.83, 1480.29 (C=C aromatic), 1365.49 (C-N stretching), 1274.24 (C-O stretching).  $^1\text{H}$  NMR (500 MHz, DMSO- $d_6$ ,  $\delta$  ppm) H: 8.90 (s, 2H, HC=N, H-7, 14), 7.63 (d, 2H,  $J = 9$  Hz,  $H_{\text{aromatic}}$ , H-1, 16), 7.40 (m, 6H,  $H_{\text{aromatic}}$ , H-3, 9, 10, 11, 12, 18), 6.93 (m, 4H,  $H_{\text{aromatic}}$ , H-2, 4, 17, 19).  $^{13}\text{C}$  NMR (125 MHz, DMSO- $d_6$ ,  $\delta$  ppm) C: 164.57 (C-5, 20), 160.91 (C-7, 14), 142.79 (C-8, 13), 132.97 (C-1, 16), 132.99 (C-9, 12), 128.35 (C-10, 11), 120.28 (C-3, 18), 120.01 (C-2, 17),

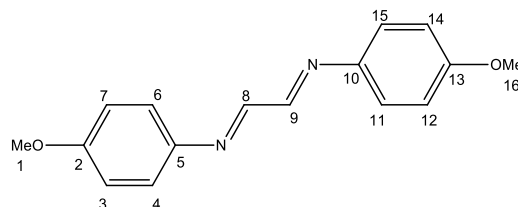
119.62 (C-6, 15), 117.20 (C-4, 19). UV-Vis (DCM) ( $\lambda_{\max}/\text{nm}$ ): 270 and 335. Anal. Calcd. For  $\text{C}_{20}\text{H}_{16}\text{N}_2\text{O}_2$ : C, 75.93; H, 5.10; N, 8.86. Found: C, 75.83; H, 4.80; N, 8.94.

*Preparation of (N<sup>1</sup>E,N<sup>2</sup>E)-N<sup>1</sup>,N<sup>2</sup>-bis(4-methoxybenzylidene)benzene-1,2-diamine, (2c)*



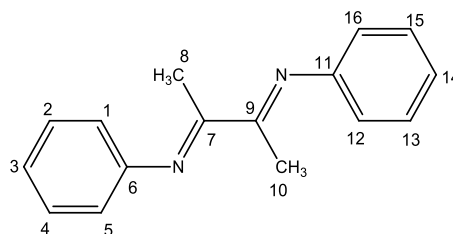
The procedure was similar to **1c** but *p*-phenylenediamine was replaced with *o*-phenylenediamine (5 mmol, 0.541 g). The solvent of the mixture solution was reduced until ~15 ml and left to precipitate at room temperature. The white precipitate formed was collected and washed with cold ethanol for a few times. Purification of the product was done *via* slow vapour diffusion of hexane into dichloromethane solution of the product. Yield: 1.549 g, 90%. IR (KBr,  $\text{cm}^{-1}$ )  $\nu$ : 3013.90 (C-H aromatic), 2831.40 (C-H vibration), 1606.87 (C=N stretching), 1509.73, 1456.75 (C=C aromatic), 1291.91 (C-N stretching), 826.82 (*para*-Subst.).  $^1\text{H}$  NMR (500 MHz,  $\text{CDCl}_3$ ,  $\delta$  ppm) H: 7.88 (s, 1H, HC=N, H-8), 7.86 (s, 1H, HC=N, H-15), 7.65 (d, 2H,  $J = 8$  Hz,  $\text{H}_{\text{aromatic}}$ , H-6, 17), 7.23 (d, 2H,  $J = 7$  Hz,  $\text{H}_{\text{aromatic}}$ , H-11, 12), 7.03 (d, 2H,  $J = 8$  Hz,  $\text{H}_{\text{aromatic}}$ , H-4, 21), 6.97 (d, 2H,  $J = 8$  Hz,  $\text{H}_{\text{aromatic}}$ , H-7, 18), 6.86 (d, 2H,  $J = 8$  Hz,  $\text{H}_{\text{aromatic}}$ , H-3, 20), 5.40 (s, 2H,  $\text{H}_{\text{aromatic}}$ , H-10, 13), 3.85 (s, 3H, H-1), 3.78 (s, 3H, H-22).  $^{13}\text{C}$  NMR (125 MHz,  $\text{CDCl}_3$ ,  $\delta$  ppm) C: 161.02 (C-2), 159.24 (C-19), 154.24 (C-8), 143.28 (C-15), 136.20 (C-9), 130.81 (C-14), 128.60 (C-5), 127.33 (C-16), 122.85 (C-11, 12), 122.64 (C-10, 13), 119.82 (C-7, 3), 114.54 (C-21, 17), 114.30 (C-20, 18), 110.54 (C-6, 4), 55.48 (C-1), 55.41 (C-22). UV-Vis (DCM) ( $\lambda_{\max}/\text{nm}$ ): 290 and 359. Anal. Calcd. For  $\text{C}_{22}\text{H}_{20}\text{N}_2\text{O}_2$ : C, 76.72; H, 5.85; N, 8.13. Found: C, 76.38; H, 5.63; N, 7.96. MS ( $m/z$ ): 344  $[\text{M}]^+$ .

*Preparation of (N,N'E,N,N'E)-N,N'-(ethane-1,2-diylidene)bis(4-methoxyaniline), (3c)*



The procedure was also similar to **1c** but *p*-phenylenediamine was replaced with glyoxal (5 mmol, 0.290 g). The dark green needle precipitate was formed and isolated *via* filtration and washed with cold ethanol few times. The product was in high purity and no purification steps needed. Yield: 1.034 g, 77%. IR (KBr,  $\text{cm}^{-1}$ )  $\nu$ : 3016.84 (C-H aromatic), 2828.45 (C-H vibration), 1603.92 (C=N stretching), 1583.31, 1492.07 (C=C aromatic), 1280.13 (C-N stretching), 816.99 (*p*-Subst.).  $^1\text{H}$  NMR (500 MHz,  $\text{CDCl}_3$ ,  $\delta$  ppm) H: 8.42 (s, 2H, H-8, 9), 7.33 (d, 4H,  $J = 7$  Hz, H-4, 6, 11, 15), 6.95 (d, 4H,  $J = 7$  Hz, H-3, 7, 12, 14), 3.84 (s, 6H, H-1, 16).  $^{13}\text{C}$  NMR (125 MHz,  $\text{CDCl}_3$ ,  $\delta$  ppm) C: 159.90 (C-2, 13), 157.72 (C-8, 9), 143.12 (C-5, 10), 123.19 (C-4, 6, 11, 15), 114.74 (C-3, 7, 12, 14), 55.67 (C-1, 16). UV-Vis (DCM) ( $\lambda_{\max}/\text{nm}$ ): 296 and 376. Anal. Calcd. For  $\text{C}_{16}\text{H}_{16}\text{N}_2\text{O}_2$ : C, 71.62; H, 6.01; N, 10.44. Found: C, 71.20; H, 5.74; N, 10.14. MS ( $m/z$ ): 267  $[\text{M}]^+$ .

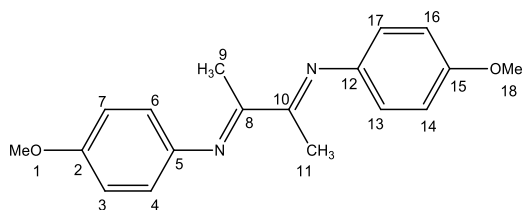
*Preparation of (N,N'E,N,N'E)-N,N'-(butane-2,3-diylidene)dianiline, (4a)*



Diacetyl (5 mmol, 0.430 g) was added into a beaker. Then, 5 drops of glacial acetic acid, aniline (10 mmol, 0.931 g) and 1 ml of ethanol was added into the beaker containing diacetyl.

The mixture was stirred at room temperature until yellow precipitate comes out. The formed precipitate was isolated *via* filtration and wash with cold ethanol and diethyl ether. Yield: 0.221 g, 18%. IR (KBr,  $\text{cm}^{-1}$ )  $\nu$ : 3061.00 (C-H aromatic), 2960.92 (C-H vibration), 1630.42 (C=N stretching), 1586.21, 1480.29 (C=C aromatic), 1366.44 (C-N stretching).  $^1\text{H}$  NMR (500 MHz,  $\text{CDCl}_3$ ,  $\delta$  ppm) H: 7.38 (t, 4H,  $J = 14$  Hz, H-2, 4, 13, 15), 7.12 (t, 2H,  $J = 15$  Hz, H-3, 14), 6.80 (d, 4H,  $J = 10$  Hz, H-1, 5, 12, 16), 2.16 (s, 6H, H-8, 10).  $^{13}\text{C}$  NMR (125 MHz,  $\text{CDCl}_3$ ,  $\delta$  ppm) C: 168.36 (C-7, 9), 151.06 (C-6, 11), 129.07 (C-2, 4, 13, 15), 123.91 (C-3, 14), 118.75 (C-1, 5, 12, 16), 15.53 (C-8, 10). UV-Vis (DCM) ( $\lambda_{\text{max}}/\text{nm}$ ): 334. Anal. Calcd. For  $\text{C}_{16}\text{H}_{16}\text{N}_2$ : C, 81.32; H, 6.82; N, 11.85. Found: C, 81.64; H, 6.47; N, 11.77. MS ( $m/z$ ): 236  $[\text{M}]^+$ .

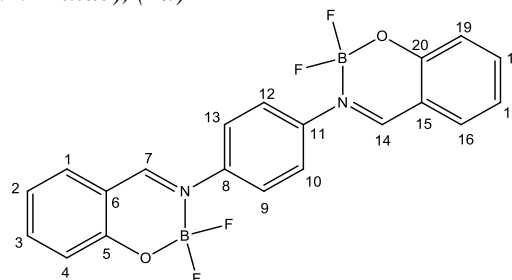
*Preparation of (N,N'E,N,N'E)-N,N'-(butane-2,3-diylidene)bis(4-methoxyaniline), (4c)*



The procedure was also similar to **1c** but *p*-phenylenediamine was replaced with diacetyl (5 mmol, 0.430 g). The dark green precipitate was form and isolated *via* filtration and washed with cold ethanol few times. The product was in high purity and no purification steps needed. Yield: 1.407 g, 95%. IR (KBr,  $\text{cm}^{-1}$ )  $\nu$ : 2999.18 (C-H aromatic), 2834.34 (C-H vibration), 1630.42 (C=N stretching), 1600.91, 1497.96 (C=C aromatic), 1353.72 (C-N stretching), 838.59 (*p*-Subst.).  $^1\text{H}$  NMR (500 MHz,  $\text{DMSO-d}_6$ ,  $\delta$  ppm) H: 6.96 (d, 4H,  $J = 9$  Hz, H-4, 6, 13, 17), 6.80 (d, 4H,  $J = 9$  Hz, H-3, 7, 14, 16), 3.76 (s, 6H, H-1, 18), 2.08 (s, 6H, H-9, 11).  $^{13}\text{C}$  NMR (125 MHz,  $\text{DMSO-d}_6$ ,  $\delta$  ppm) C: 168.61 (C-2, 15), 156.55 (C-8, 10), 144.19 (C-5, 12), 120.70 (C-4, 6, 13, 17), 114.39 (C-3, 7, 14, 16), 55.61 (C-1, 18), 15.55 (C-9, 11). UV-Vis (DCM) ( $\lambda_{\text{max}}/\text{nm}$ ): 291 and 354. Anal. Calcd. For  $\text{C}_{18}\text{H}_{20}\text{N}_2\text{O}_2$ : C, 72.95; H, 6.80; N, 9.45. Found: C, 73.35; H, 6.52; N, 9.03. MS ( $m/z$ ): 296  $[\text{M}]^+$ .

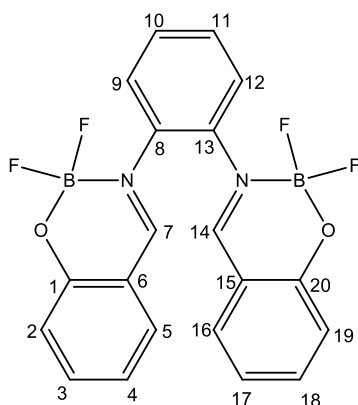
**Preparation of Symmetrical bis-Schiff Base with Boron Complex**

*Preparation of 3,3'-(1,4-phenylene)bis(2,2-difluoro-2H-benzo[e][1,3,2]oxazaborinin-3-ium-2-uide), (1d)*



Compound **1b** (0.63 mmol, 0.199 g) in 30 ml of dry dichloromethane was added into round bottom flask. Then, triethylamine (6.3 mmol, 0.637 g) was added into the solution. The mixture was degassed *via* freeze-pump-thaw technique and added with nitrogen gas and stirred for 15 min at 50 °C. After that, boron difluoride diethyl ether (12.6 mmol, 1.788 g) was added slowly *via* syringe and degassed the mixture again *via* freeze-pump-thaw technique. The mixture was then refluxed while stirred for 4 hr at 85 °C to afford bright yellow precipitate. The formed precipitate was collected *via* filtration and washed with water and diethyl ether 15 mL each time for several times. Yield: 0.219 g, 84%. IR (KBr,  $\text{cm}^{-1}$ )  $\nu$ : 3069.83 (C-H aromatic), 3037.45 (C-H vibration), 1618.64 (C=N stretching), 1550.94, 1503.84 (C=H aromatic), 1315.45 (C-N stretching), 1212.43, 1044.64 (B-F), 1153.56, 1097.63 (B-O). UV-Vis (DCM) ( $\lambda_{\text{max}}/\text{nm}$ ): 293 and 38297, 385 and 442. Anal. Calcd. For  $\text{C}_{20}\text{H}_{14}\text{B}_2\text{F}_4\text{N}_2\text{O}_2$ : C, 58.31; H, 3.43; N, 6.80. Found: C, 58.34; H, 3.09; N, 6.66.

*Preparation of 3,3'-(1,2-phenylene)bis(2,2-difluoro-2H-benzo[e][1,3,2]oxazaborinin-3-ium-2-uide), (2d)*



The procedure was similar to **1d** but ligand **2b** (0.63 mmol, 0.199 g) was used instead of ligand **1b**. The bright yellow precipitate was formed and collected *via* filtration and washed for a few times by using water and diethyl ether. Yield: 0.236 g, 91%. IR (KBr,  $\text{cm}^{-1}$ ): 3078.66 (C-H aromatic), 3046.28 (C-H vibration), 1621.59 (C=N stretching), 1553.88, 1474.41 (C-H aromatic), 1383.16 (C-N stretching), 1218.32, 1062.31 (B-F), 1130.01, 1085.85 (B-O). UV-Vis (DCM) ( $\lambda_{\text{max}}/\text{nm}$ ): 279 and 364. Anal. Calcd. For  $\text{C}_{20}\text{H}_{14}\text{B}_2\text{F}_4\text{N}_2\text{O}_2$ : C, 58.31; H, 3.43; N, 6.80. Found: C, 57.95; H, 3.05; N, 6.66.

### Fabrication of Dye-Sensitized Solar Cell (DSSC)

The DSSC fabrication procedure was done referring to method published by Phan *et al.*, (2019) and Alhorani *et al.* (2021) with some modifications. The details of the preparation method can be found in supplementary materials.

Titanium (IV) oxide coated fluoride doped tin oxide (FTO) glass was used as the working electrode and indium tin oxide (ITO) glass was coated with electric paint containing carbon black and graphene were used as the counter electrode. The complete assembly of DSSC device is shown in Figure 2.

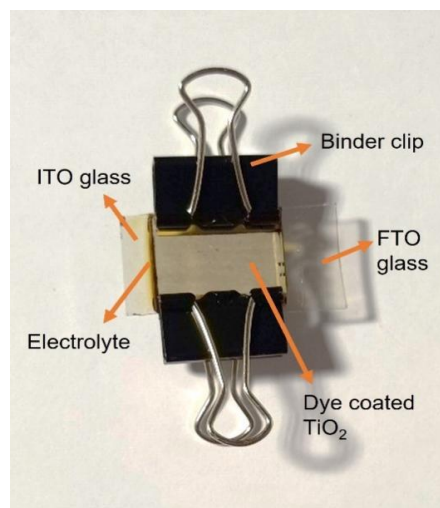


**Figure 2.** Complete assembly of DSSC device

### Photoelectrochemical Measurement

Prior to testing the bis-Schiff base ligands and its boron complexes, *cis*-bis(isothiocyanato)bis(2,2'-bipyridyl-4,4'-dicarboxylato) ruthenium(II), commonly known as N3 dye was tested in order to make sure that the fabrication method and measurements were correct and consistent. The fabricated DSSC were tested with 100W LED lamp with resistor box (Shanghai Domao; Model: ZX21) and multimeter (XEOLE, China; Model: XL830L) to record the current-voltage (J-V) characteristics. An arrangement of 31.6 cm x 28.6 cm x 23.8 cm box was made for the measurements. Light intensity of the LED lamp was measured using light meter (Sunche Light Meter HS 1010) at the cell location point meanwhile the active area of the cell ( $2\text{ cm}^2$ ) was measured with a ruler.

From the J-V curves, the fill factor (FF) the power conversion efficiency ( $\eta\%$ ) of the cell was calculated using the equation as shown in Eq. (1) and Eq. (2), respectively:

$$FF = \frac{J_{MP} \times V_{MP}}{J_{SC} \times V_{OC}} \quad \text{Eq. (1)}$$

where;  $J_{MP}$  = maximum current (mA),  $V_{MP}$  = maximum voltage (mV),  $J_{SC}$  = short-circuit currents (mA),  $V_{OC}$  = open-circuit voltages (mV).

$$\eta = \frac{J_{sc} \times V_{oc} \times FF}{P_{in}} \times 100\% \quad \text{Eq. (2)}$$

where;  $J_{sc}$  = solar circuit current density ( $\text{mA}/\text{cm}^2$ ),  $V_{oc}$  = open circuit photovoltage (V),

$FF$  = fill factor (%),  $P_{in}$  = incident light intensity ( $W/cm^2$ ),  $\eta$  = power conversion efficiency (%).

## RESULTS AND DISCUSSION

The symmetrical bis-Schiff base compounds were successfully synthesized except for compounds named **3a**, **3b** and **4b** as shown in Figure 3. The synthesis of Compound **3a** failed because of the instability of imine (C=N) bond. The instability of imine bond causes the hydrolysis of the structure which made the

starting materials still present in the final product. Several purification techniques were done however, the starting materials still present in the product. The formation of by-products instead of Schiff base in the synthesis of **3b** and **4b** was the reason causing the failure to synthesize these two compounds. This is because they undergo cyclization with the -OH substituent forming bibenzoxazoline. The spectroscopic data on these compounds can be found in Figure S9 – S12.

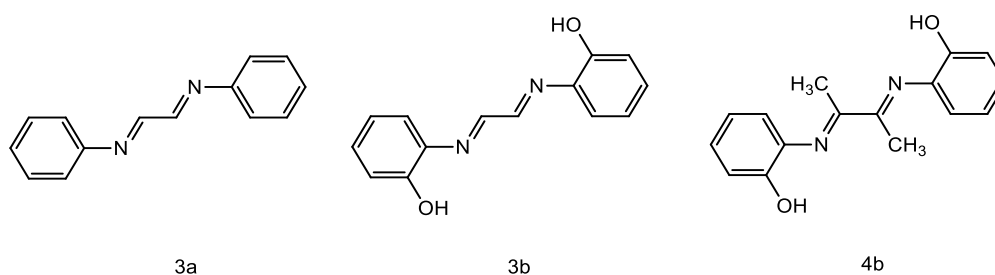


**Figure 3.** Molecular structure of **3a**, **3b**, and **4b**

The yields and elemental data for all compounds are tabulated in Table 1. All compounds show satisfying yield except for compounds **2a** and **4a** due to the loss while washing the precipitate. The unreacted starting materials still appeared with the product and can be removed with washing. However, compound **4a** is soluble in most of organic solvent thus explained the loss of its product during washing. In addition, the purity of all compounds was ensured by elemental analysis results, with all compounds showing differences of 0.4% between calculated and found results.

The formation of symmetrical bis-Schiff base compounds was confirmed mainly by the disappearance of C=O peak at around  $1750 - 1700\text{ cm}^{-1}$  in the IR spectrum (Table 2) of the starting materials. Apart from that, the  $NH_2$  peak

from the starting material was absent at around  $1681\text{ cm}^{-1}$  region. Meanwhile, a new stretching band was found around  $1630 - 1600\text{ cm}^{-1}$  which is attributed to C=N bond in a Schiff base structure. In addition, a broad band was found at around  $3300\text{ cm}^{-1}$  due to the -OH group that presents at the *ortho* position of the phenyl ring in the compounds **1b** and **2b**. Due to the presence of -N=C-C=N- conjugation system along the molecule that facilitates the electron delocalization, the frequencies were found to be shifted to lower frequencies (Pavia *et al.*, 2001). Furthermore, the peak at around  $800\text{ cm}^{-1}$  was also found in compounds **1c**, **2c**, **3c** and **4c** which attributed to the *para*- position -OMe substituent at both sides of the phenyl rings. Figure 4 shows the IR spectrum of **1a** meanwhile IR spectra for other compounds can be found in Figure S3 – S14.

**Table 1.** Yields and elemental data for symmetrical bis-Schiff base compounds

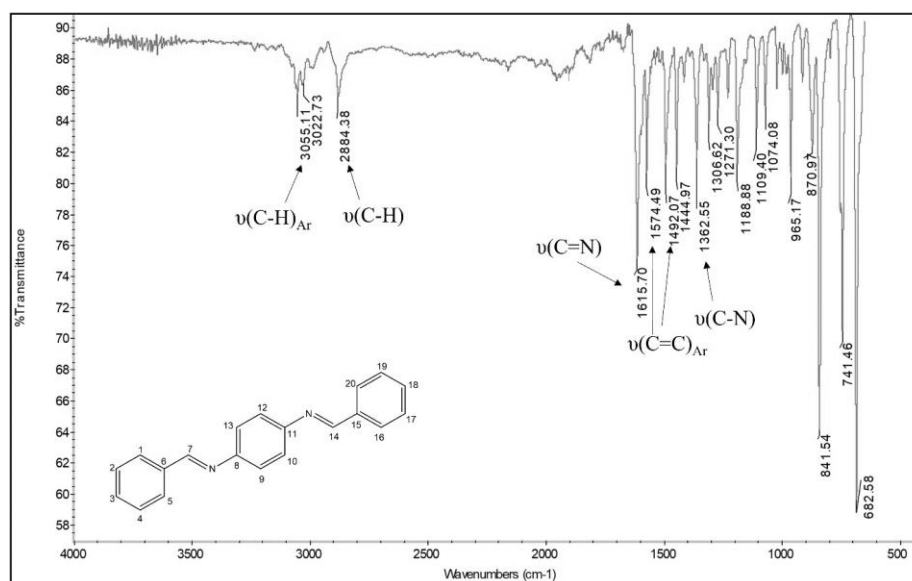
Compound	Formula	Yield (%)	Found (Calculated)		
			C%	H%	N%
<b>1a</b>	$C_{20}H_{16}N_2$	98	84.43 (84.48)	5.53 (5.67)	9.62 (9.85)
<b>1b</b>	$C_{20}H_{16}N_2O_2$	95	75.72 (75.93)	4.95 (5.10)	8.74 (8.86)
<b>1c</b>	$C_{22}H_{20}N_2O_2$	97	76.84 (76.72)	5.71 (5.85)	7.74 (8.13)
<b>1d</b>	$C_{20}H_{14}B_2F_4N_2O_2$	84	58.31 (58.34)	3.43 (3.09)	6.80 (6.66)
<b>2a</b>	$C_{20}H_{16}N_2$	54	84.03 (84.48)	5.67 (5.67)	10.08 (9.85)
<b>2b</b>	$C_{20}H_{16}N_2O_2$	92	75.83 (75.93)	4.80 (5.10)	8.94 (8.86)
<b>2c</b>	$C_{22}H_{20}N_2O_2$	90	76.38 (76.72)	5.63 (5.85)	7.96 (8.13)

<b>2d</b>	C <sub>20</sub> H <sub>14</sub> B <sub>2</sub> F <sub>4</sub> N <sub>2</sub> O <sub>2</sub>	91	58.31 (57.95)	3.43 (3.05)	6.80 (6.66)
<b>3c</b>	C <sub>16</sub> H <sub>16</sub> N <sub>2</sub> O <sub>2</sub>	97	71.20 (71.62)	5.74 (6.01)	10.14 (10.44)
<b>4a</b>	C <sub>16</sub> H <sub>16</sub> N <sub>2</sub>	18	81.64 (81.32)	6.47 (6.82)	11.77 (11.85)
<b>4c</b>	C <sub>18</sub> H <sub>20</sub> N <sub>2</sub> O <sub>2</sub>	95	73.35 (72.95)	6.52 (6.80)	9.03 (9.45)

**Table 2.** Selected IR frequencies of **1a** – **4c**

Comp.	$\nu$ OH	$\nu$ C=N	$\nu$ C=C <sub>ar</sub>	$\nu$ B-F	$\nu$ B-O	$\nu$ ( <i>p</i> -Subst.)
<b>1a</b>	NA	1616	1575 & 1492	NA	NA	NA
<b>1b</b>	3375	1600	1568 & 1485	NA	NA	NA
<b>1c</b>	NA	1604	1569 & 1510	NA	NA	844
<b>1d</b>	NA	1619	1551 & 1504	1212 & 1045	1154 & 1098	NA
<b>2a</b>	NA	1603	1488 & 1447	NA	NA	NA
<b>2b</b>	3320	1607	1557 & 1480	NA	NA	NA
<b>2c</b>	NA	1607	1510 & 1457	NA	NA	827
<b>2d</b>	NA	1622	1554 & 1474	1218 & 1062	1130 & 1086	NA
<b>3c</b>	NA	1627	1589 & 1489	NA	NA	817
<b>4a</b>	NA	1630	1586 & 1480	NA	NA	NA
<b>4c</b>	NA	1630	1601 & 1498	NA	NA	839

\*NA = Not available

**Figure 4.** IR spectrum of symmetrical bis-Schiff base of compound **1a**

<sup>1</sup>H (Table 3) and <sup>13</sup>C NMR data (Table 4) can also serve as strong evidence to confirm the structures. The formation of Schiff base compounds was confirmed by the absence of CHO signal at around 10 ppm and the appearance of HC=N signal at the range of  $\delta$ H 7.88 –  $\delta$ H 9.03 ppm which indicates the successful formation of diimine compound.

Moreover, all other aromatic protons' signals were found at the range of 6 ppm – 7 ppm corresponding to their structure. In addition, compounds **1c**, **2c**, **3c** and **4c** have an extra singlet signal at  $\delta$ H 3.76 –  $\delta$ H 3.84 ppm attributed to the *para*-substituted methoxy group of the aromatic ring. Besides, compounds **4a** and **4b** recorded an important singlet signal at

2.16 ppm and 2.08 ppm respectively which was assigned to the methyl group hydrogen ( $H_3C-C=N$ ) of attached at the  $\pi$ -spacer of both compounds. The  $^1H$  spectrum of compound **1a** is shown in Figure 5, meanwhile the  $^1H$  spectra of other compounds can be found in supplementary materials. As for the  $^{13}C$  NMR spectra, all signals found were correct according to their respective structure. However, NMR data for compounds **1d** and **2d** failed to be obtained due to low solubility in organic solvents. The

evaluation of the deprotonation of hydroxyl groups can be confirmed with FTIR data where -OH peak disappeared after complexation. Due to NMR analysis for compound **1d** and **2d** cannot be obtained, the structure arrangement for both compounds whether they are symmetrical or not symmetrical cannot be confirmed further. Nevertheless, the data obtained from IR, UV-Visible and CHN analysis showed the correct data according to their structure thus proving the successful formation of **1d** and **2d**.

**Table 3.**  $^1H$  NMR data of symmetrical bis-Schiff base compounds **1a-4c**

Comp.	$\delta$ HC=N	$\delta$ H aromatic	$\delta$ OCH <sub>3</sub>	$\delta$ CH <sub>3</sub>
<b>1a</b>	8.69	7.96 (d,4H), 7.53 (m,6H), 7.37 (s,4H)	NA	NA
<b>1b</b>	9.03	7.68 (d, 2H), 7.55 (s, 4H), 7.55 (s, 4H), 7.43 (t, 2H), 6.99 (m, 4H)	NA	NA
<b>1c</b>	8.59	7.90 (d, 4H), 7.30 (s, 4H), 7.08 (d, 4H)	3.84 (s, 6H)	NA
<b>2a</b>	7.88, 7.87	7.69 (d, 2H), 7.45 (m, 4H), 7.26 (m, 6H), 7.09 (d, 2H)	NA	NA
<b>2b</b>	8.90	7.63 (d, 2H), 7.40 (m, 6H), 6.93 (m, 4H)	NA	NA
<b>2c</b>	7.88, 7.86	7.65 (d, 2H), 7.23 (d, 2H), 7.03 (d, 2H), 6.97 (d, 2H), 6.86 (d, 2H), 5.40 (s, 2H)	3.85 (s, 3H), 3.78 (s, 3H)	NA
<b>3c</b>	8.42	7.33 (d, 4H), 6.95 (d, 4H)	3.84 (s, 6H)	NA
<b>4a</b>	NA	7.38 (t, 4H), 7.12 (t, 2H), 6.80 (d, 4H)	NA	2.16 (s, 6H)
<b>4c</b>	NA	6.96 (d, 4H), 6.80 d, 4H)	3.76 (s, 6H)	2.08 (s, 6H)

\*NA = Not available

**Table 4.**  $^{13}C$  NMR data of symmetrical bis-Schiff base compounds **1a-4c**

Comp.	$\delta$ C-OH	$\delta$ C=N	$\delta$ C-N	$\delta$ C=C	$\delta$ C-OCH <sub>3</sub>	$\delta$ OCH <sub>3</sub>	$\delta$ C-CH <sub>3</sub>
<b>1a</b>	NA	160.62	149.99	136.61, 131.90, 129.30, 129.11, 122.44	NA	NA	NA
<b>1b</b>	163.74	160.82	147.15	133.90, 133.00, 123.10, 119.90, 119.75, 117.06	NA	NA	NA
<b>1c</b>	NA	160.00	133.02	131.54, 130.26, 122.77, 115.22	163.26	56.45	NA
<b>2a</b>	NA	154.16, 142.88	136.40, 136.06	130.17, 129.91, 129.41, 129.21, 128.93, 127.66, 126.09, 123.31, 122.98, 119.99, 110.72	NA	NA	NA
<b>2b</b>	164.57	160.91	142.79	132.97, 132.99, 128.35, 120.28, 120.01, 119.62, 117.20	NA	NA	NA
<b>2c</b>	NA	154.24, 143.28	136.20, 130.81	128.60, 127.33, 122.85, 122.64, 119.82, 114.54, 114.30, 110.54	161.02, 159.24	55.48, 55.41	NA
<b>3c</b>	NA	157.72	143.12	123.19, 114.74	159.90	55.67	NA
<b>4a</b>	NA	168.36	151.06	129.07, 123.91, 118.75	NA	NA	15.53
<b>4c</b>	NA	156.55	144.19	120.70, 114.39	168.61	55.61	15.55

\*NA = Not available

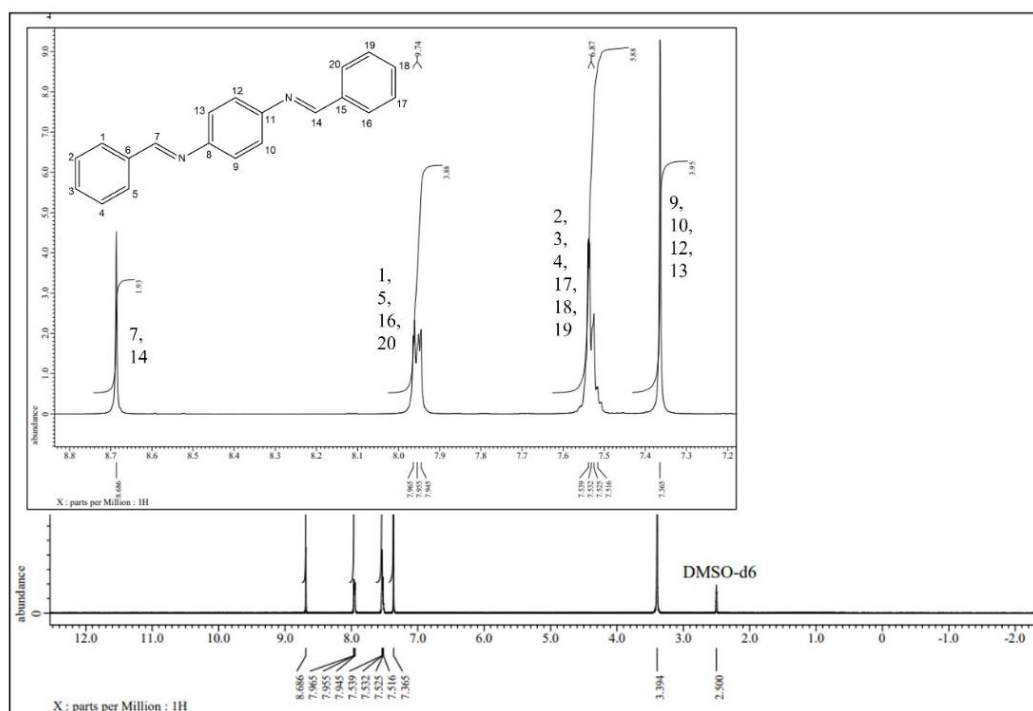


**Figure 5.**  $^1\text{H}$  NMR spectrum of compound **1a**

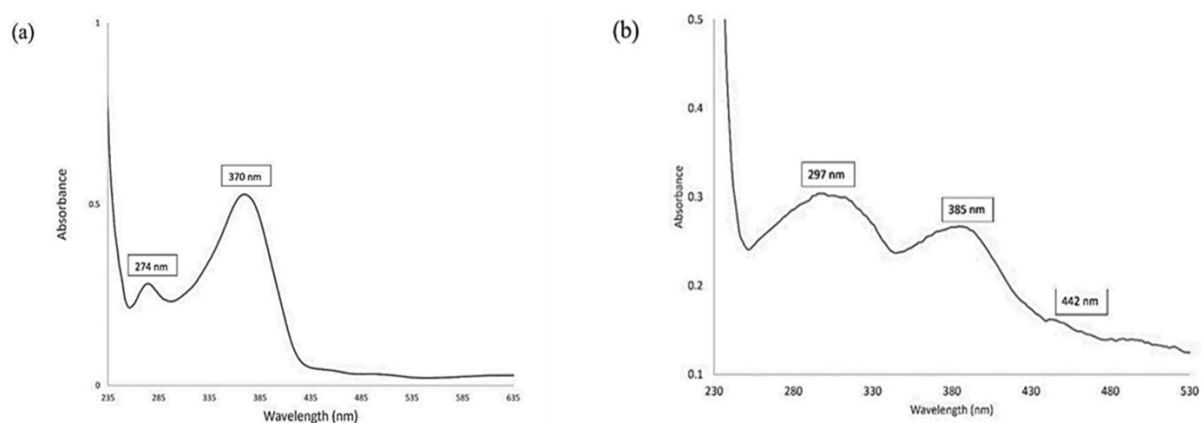


**Figure 6.** UV spectrum of compound **1b** (a) and compound **1d** (b)

UV spectrum in Figure 6 shows the difference between before (**1b**) and after (**1d**) complexation with boron difluoride. Significant absorption bands in the range of 245 – 296 nm, attributed to  $\pi \rightarrow \pi^*$  electronic transition of aromatic rings can also be seen in the absorption spectra of these compounds (Table 5). Meanwhile, the absorption bands between 296 - 376 nm, are attributed to the  $n \rightarrow \pi^*$  of the electronic transition of the azomethine group ( $-\text{C}=\text{N}-$ ) (Alattar *et al.*, 2020). Indeed, the absorption bands shifted to a longer wavelength due to the conjugation effects ( $-\text{N}=\text{C}-\text{C}=\text{N}-$ ). Apart from these two bands, new band was found in compounds **1d** and **2d** at 442 and 449

nm, respectively, due to intermolecular charge transfer (ICT).

GC-MS data (Figure 7) also shows all compounds were pure with only one peak with

corresponding base peak in the chromatogram. But for compound **2b**, it underwent hydrolysis in high temperature, hence two peaks were found.

**Table 5.** UV-Visible data of symmetrical bis-Schiff base compounds **1a** – **4c**

Comp	$\pi \rightarrow \pi^*$ (nm)	$n \rightarrow \pi^*$ (nm)	Intermolecular charge transfer (ICT) (nm)
------	---------------------------------	-------------------------------	--

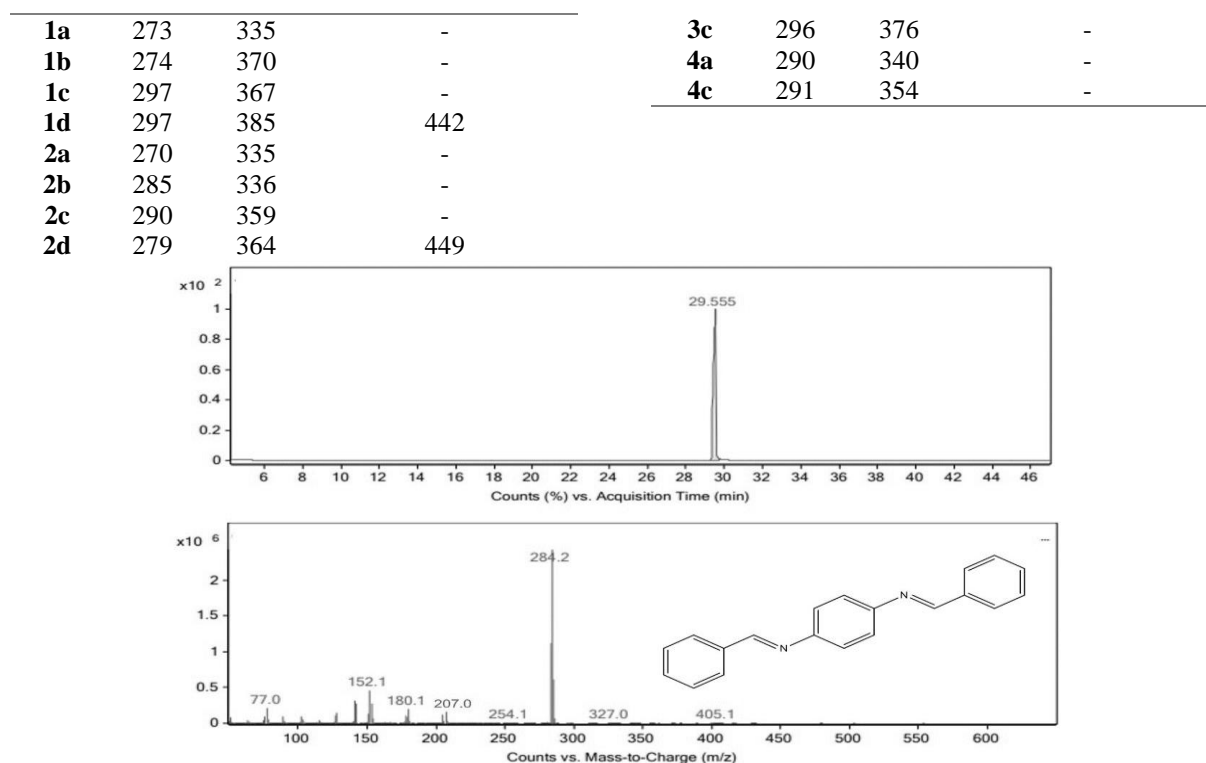


**Figure 7.** Gas chromatogram and mass spectrum of compound **1a**

### Application of Symmetrical bis-Schiff Base Compounds and Complexes in DSSC

All the successfully synthesized symmetrical bis-Schiff base compounds and  $\text{BF}_2$  complexes that have been discussed previously were applied as dye-sensitizer in DSSC devices. It is worth noting that the DSSC performance

efficiency was calculated with respect to 100W LED light source not to the standard solar simulator AM 1.5G under an incident light intensity of  $100 \text{ mW/cm}^2$ . In an arrangement of  $31.6 \text{ cm} \times 28.6 \text{ cm} \times 23.8 \text{ cm}$  box, a LED light, and DSSC device connected to resistor box and multimeter were arranged as shown in Figure 8.

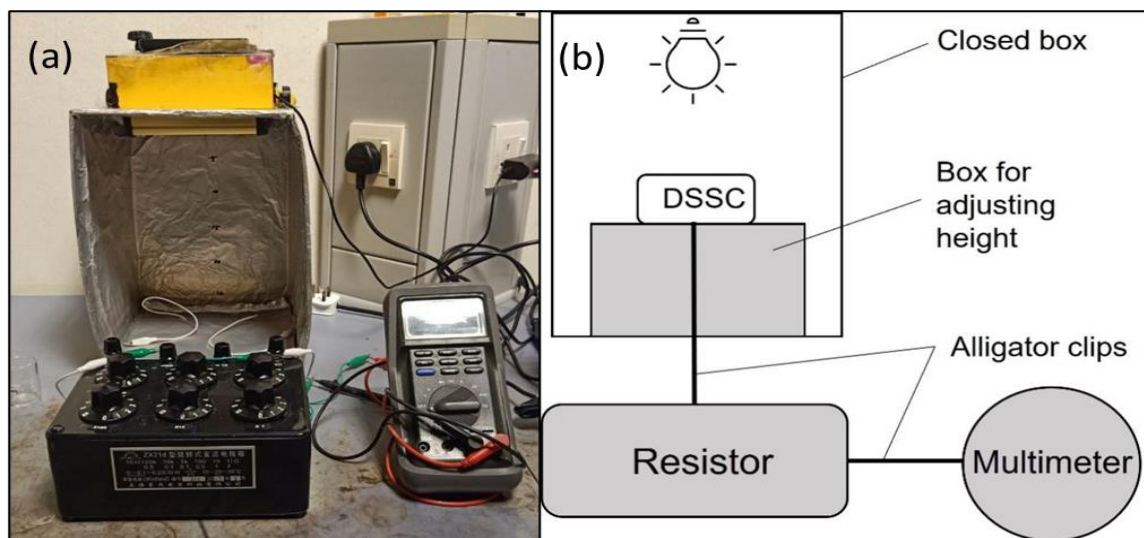


**Figure 8.** (a) Arrangement of photoelectrical measurement and (b) schematic diagram of dye sensitized solar cell (DSSC)

The current-voltage ( $J$ - $V$ ) and power-voltage ( $P$ - $V$ ) curves were calculated and generated from the data obtained (Figure 9). From these curves, the value of short-circuit currents ( $J_{SC}$ ), open-circuit voltages ( $V_{OC}$ ), maximum current ( $J_{MP}$ )

and maximum voltage ( $V_{MP}$ ) were calculated. Meanwhile, the value of fill factor ( $FF$ ) and efficiency ( $\eta\%$ ) was calculated using Eq. (1) and (2), respectively.

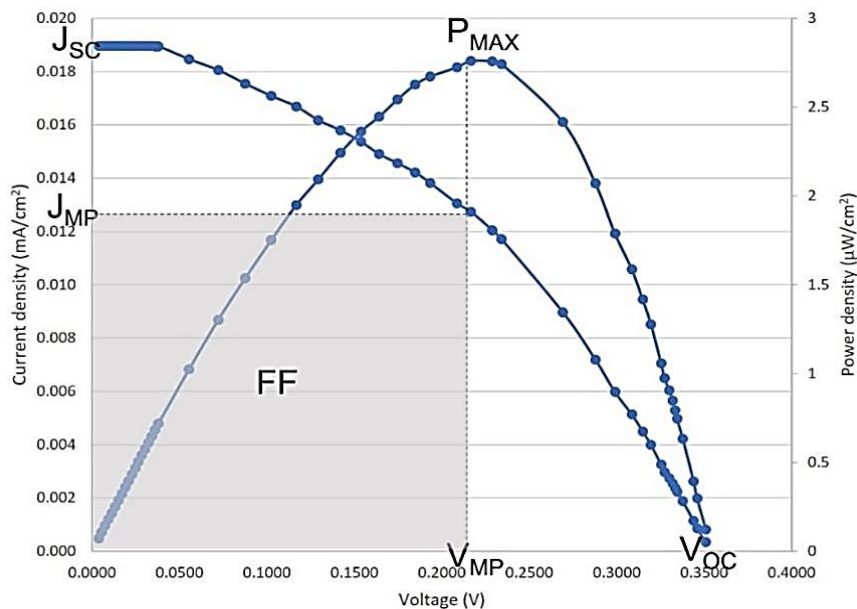


**Figure 9.** Current and power vs voltage curves of N3 dye sensitizer

From the efficiency formula, the incident light intensity ( $P_{in}$ ) is usually measured using irradiance (lux). However, rather than irradiance, illuminance is the better way to quantify the light level for indoor environment but somehow illuminance creates conversion problems. This is because there is still no simple and easily obtained standard method to convert illuminance (lux) into irradiance ( $W.m^{-2}$ ) and *vice versa* (Michael *et al.*, 2020). To convert, the different conversion factor is needed for every wavelength which can be determined from the spectral analysis of light composition. Unless the spectral composition of the light is known, it is not possible to make a conversion. Therefore, in order to get an approximate conversion factor for the incident light conversion in the formula, a wavelength is needed. As there is no equipment available to measure the exact wavelength of the light used, therefore the wavelength of the visible spectrum was used because illuminance only considers the spectrum of visible light. Given that the visible spectrum has the maximum peak at around 555 nm, as well as the peak of the eye-sensitivity curve particularly at 555 nm, the spectral irradiance of most indoor

approximately around 550 nm (Alhorani *et al.*, 2021). Therefore, for this wavelength, the corresponding value is  $1.464 \text{ mW/m}^2$ , in which the conversion rule can be extracted as shown in Eq. (3) for efficiency calculations:

$$I_{IN} \text{ (W/m}^2\text{)} = 1.464 \times 10^{-3} \times I_{IN} \text{ (lx)} \quad \text{Eq. (3)}$$

where;  $I_{IN}$  = incident light intensity.

Based on the UV spectrum of symmetrical bis-Schiff base compounds and its complex, the absorption at around 550 nm wavelength. However, the dye does gives values when tested with DSSC device meaning that the light also emits wavelength in the dye range. Therefore, as mentioned earlier, as there is no equipment to get the exact wavelength, only an approximate conversion factor can be used. The power conversion efficiency results are presented in Table 6 and the  $J/V$  curves for each series are shown in Figure 10. Each series are divided into different  $\pi$ -spacer used at the centre where (a) *p*-phenylenediamine, (b) *o*-phenylenediamine, (c) glyoxal & (d) diacetyl.

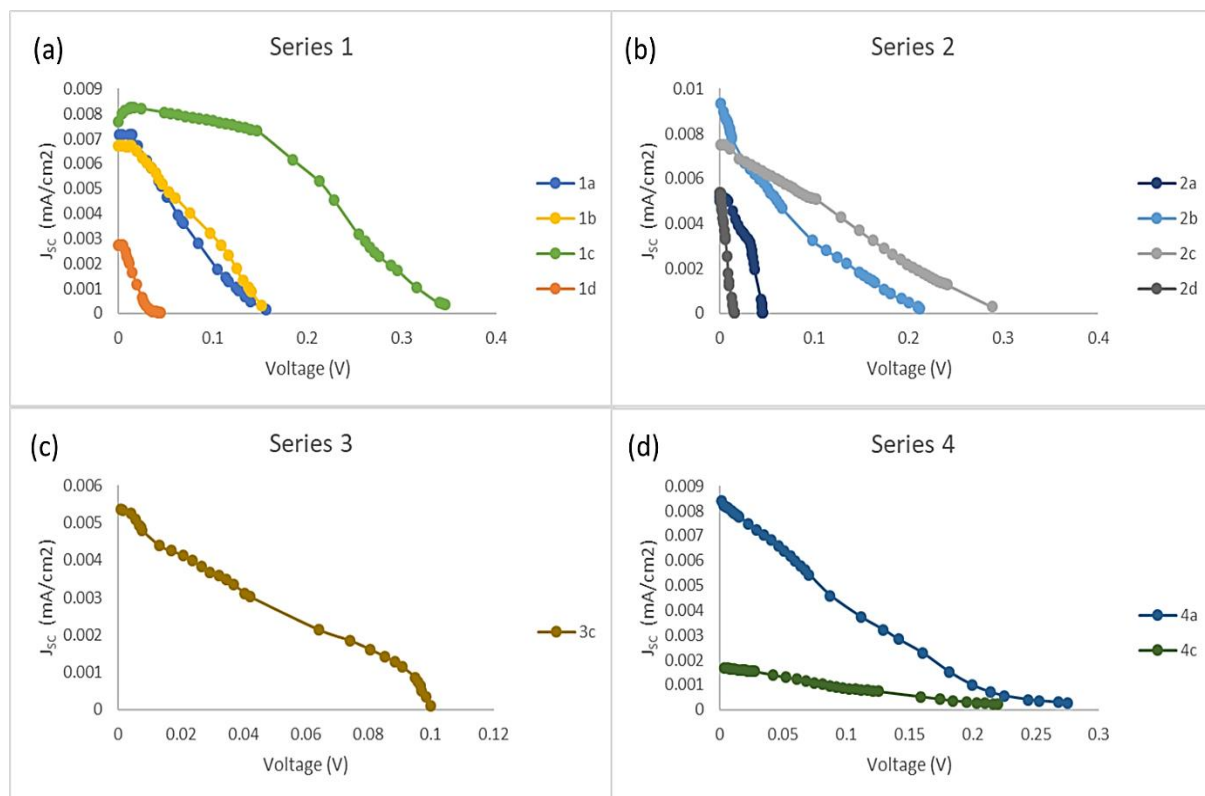


**Figure 10.**  $J/V$  measurement of symmetrical bis-Schiff base compounds and complexes as dye-sensitizer (Series are divided into different  $\pi$ -spacer used at the centre where, (a) *p*-phenylenediamine, (b) *o*-phenylenediamine, (c) glyoxal and (d) diacetyl)

From the results obtained (Table 6), compound **1c** achieved the highest power conversion efficiency (PCE) of 0.0691% with a current density of 0.0077 mA/cm<sup>2</sup>,  $V_{OC}$  of 0.3453 V and FF value of 42.9. Conversely, compound **2d** shows the lowest PCE of 0.0012%, the current density of 0.0053 mA/cm<sup>2</sup>,  $V_{OC}$  of 0.0159 V and FF of 22.8. The thickness of TiO<sub>2</sub>, the electrolyte, the cell resistance, and the conversion of photocurrent absorbed by the dye are all elements that can influence the FF value. As a result of the dye sensitizer's improved absorption, more photons are absorbed, resulting in a higher photocurrent that can be delivered to the nanocrystalline TiO<sub>2</sub> layer, increasing overall performance (Teo *et al.*, 2017). Compound **1c** shows the highest power due to the efficient electron delocalization throughout its structure as well as the presence of a good electron donor (-OMe) while compound **2d** shows the least efficiency might be due to the difficulty of the dye to absorb itself to the TiO<sub>2</sub> surface because of its solubility problem in a solvent system. Due to its poor solubility problem in a solvent system, only a little amount of dissolved dye was absorbed to the surface. Thus, causing the low efficiency.

The effect of different substituents can be observed through PCE values of the compound series 1 and series 2 (Figure 11). Compound **1c** and **2c** containing methoxy (-OMe) substituent shows the highest efficiency for both series with 0.0691% (0.0077 mA/cm<sup>2</sup>) and 0.0329% (0.0075 mA/cm<sup>2</sup>) PCE respectively. On the other hand, compounds **1b** and **2b** containing hydroxy (-OH) substituent show lower PCE compared to -OMe substituent at 0.0200% (0.0067 mA/cm<sup>2</sup>) and 0.0189% (0.0093 mA/cm<sup>2</sup>) respectively. Indeed, compounds with no substituent (**1a** and **2a**) shows the lowest PCE of 0.0166% (0.0072 mA/cm<sup>2</sup>) and 0.0060% (0.0050 mA/cm<sup>2</sup>) respectively. This can be explained in terms of electron donor strength, -OMe is a stronger electron donor than -OH. According to reports, introducing the appropriate electron donors can change how well the PCE values perform. This is due to the fact that the electron donor's ability to donate electrons can have an impact on both the HOMO values as well as the distribution of electron densities within the dye structure (Tai *et al.*, 2011; Ladomenou *et al.*, 2014).

Boron difluoride complexes (**1d** and **2d**) showed much lower PCE at 0.0017% (0.0027

mA/cm<sup>2</sup>) and 0.0012% (0.0053 mA/cm<sup>2</sup>) of PCE respectively in comparison of its free ligand of compounds **1b** and **2b**. The poor solubility of these complexes in solvent system may be the cause of low efficiency. They are only slightly soluble in a very large amount of solvents (~0.001g in 10 ml DCM) even after heating and sonicating for more than 6 hours. The

reformation of precipitates on top of the TiO<sub>2</sub> layer during the fabrication process caused the increase in thickness of the layer of working electrode as well as increased the direct contact of a working electrode with counter electrode which resulted in the increase of cell resistance affecting the efficiency of the cell (Teo *et al.*, 2017).

**Table 6.** Power conversion efficiency results of symmetrical bis-Schiff base ligands and boron difluoride complexes compounds **1a-4c**

Dye Sensitizer	I <sub>IN</sub> (lx)	I <sub>IN</sub> (W/m <sup>2</sup> )	J <sub>SC</sub> (mA/cm <sup>2</sup> )	V <sub>OC</sub> (V)	J <sub>MP</sub> (mA/cm <sup>2</sup> )	V <sub>MP</sub> (V)	FF	η%
<b>N3 dye</b>	112400	164.5536	0.0190	0.3510	0.0120	0.2289	41.4	0.1676
<b>1a</b>	102500	150.0600	0.0072	0.1560	0.0036	0.0687	22.2	0.0166
<b>1b</b>	107100	156.7944	0.0067	0.1511	0.0032	0.0969	30.9	0.0200
<b>1c</b>	112300	164.4072	0.0077	0.3453	0.0062	0.1846	42.9	0.0691
<b>1d</b>	101100	148.0104	0.0027	0.0444	0.0017	0.0149	20.3	0.0017
<b>2a</b>	114500	167.6280	0.0050	0.0453	0.0032	0.0317	44.4	0.0060
<b>2b</b>	114800	168.0672	0.0093	0.2119	0.0033	0.0977	16.1	0.0189
<b>2c</b>	113300	165.8712	0.0075	0.2877	0.0043	0.1280	25.3	0.0329
<b>2d</b>	108100	158.2584	0.0053	0.0159	0.0033	0.0059	22.8	0.0012
<b>3c</b>	114000	166.8960	0.0054	0.1000	0.0019	0.0741	25.6	0.0082
<b>4a</b>	112500	164.7000	0.0084	0.2751	0.0037	0.1118	18.0	0.0253
<b>4c</b>	112700	164.9928	0.0017	0.2200	0.0007	0.1257	24.9	0.0056

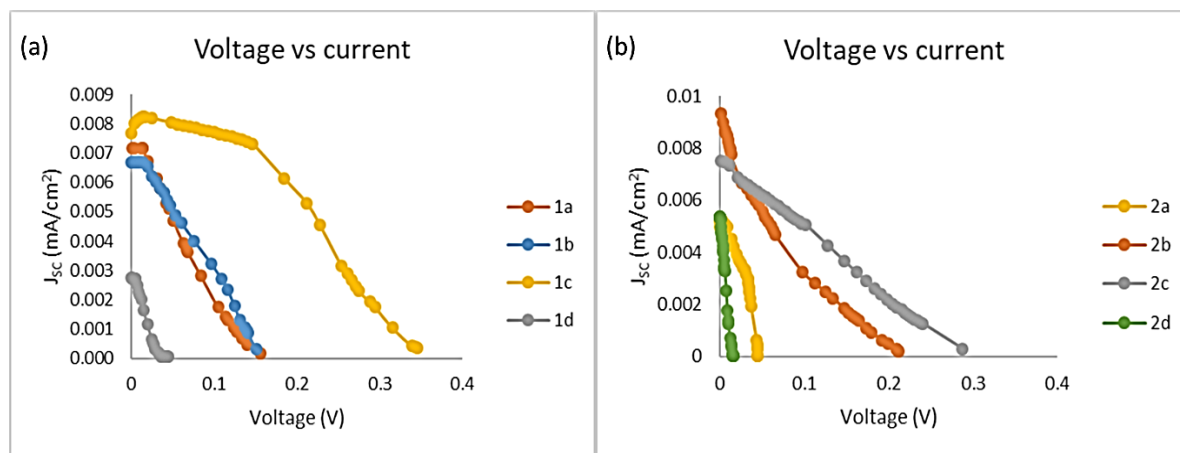


**Figure 11.** *J/V* measurement of series 1 compounds (a) and series 2 compounds (b)

In addition, the effect of the different  $\pi$ -spacer bridges can also be observed. Referring to the *J/V* measurement in Figure 12, compounds **1c** (0.0691%, 0.0077 mA/cm<sup>2</sup>) and **2c** (0.0329%, 0.0075 mA/cm<sup>2</sup>) with aromatic rings as the  $\pi$ -spacer show better PCE values compared to compound **3c** (0.0082%, 0.0054 mA/cm<sup>2</sup>) and **4c** (0.0056%, 0.0017 mA/cm<sup>2</sup>) that have non-aromatic as the  $\pi$ -spacer bridge. The conjugate

effect and the ligand flexibility in coordination structures are thought to be major factors influencing the catalytic activity of compounds (Wang *et al.*, 2003). A fused aromatic ring system is preferred over a linear chain system with rotatable single bonds to maintain strong contact through the  $\pi$ -conjugated system (Houjou *et al.*, 2017).

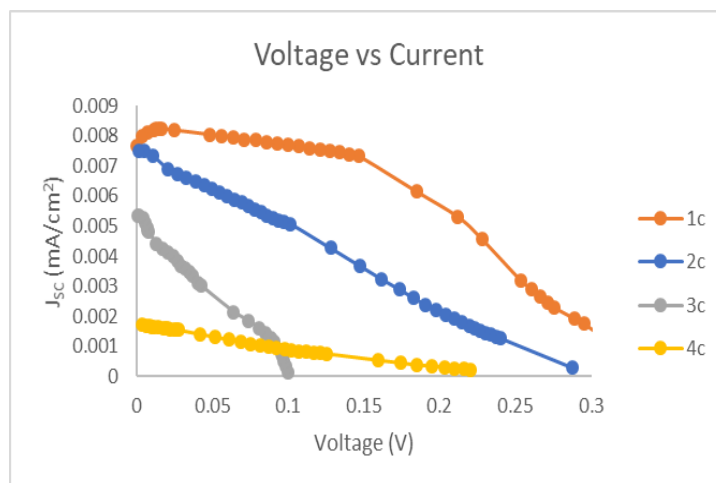


**Figure 12.**  $J/V$  measurement of symmetrical bis-Schiff base with different  $\pi$ -spacer bridge

Indeed, there have been some works of literature that have compared the  $\pi$ -conjugation effect in *ortho*-, *para*- and *meta*- position phenyl backbone of a molecule (Figure 13). It is reported that the strength of electron

delocalization through *para*-position phenyl bridge is better followed by *ortho*-position and then lastly *meta*-position phenyl bridge (Ruiz-Carretero *et al.*, 2014).

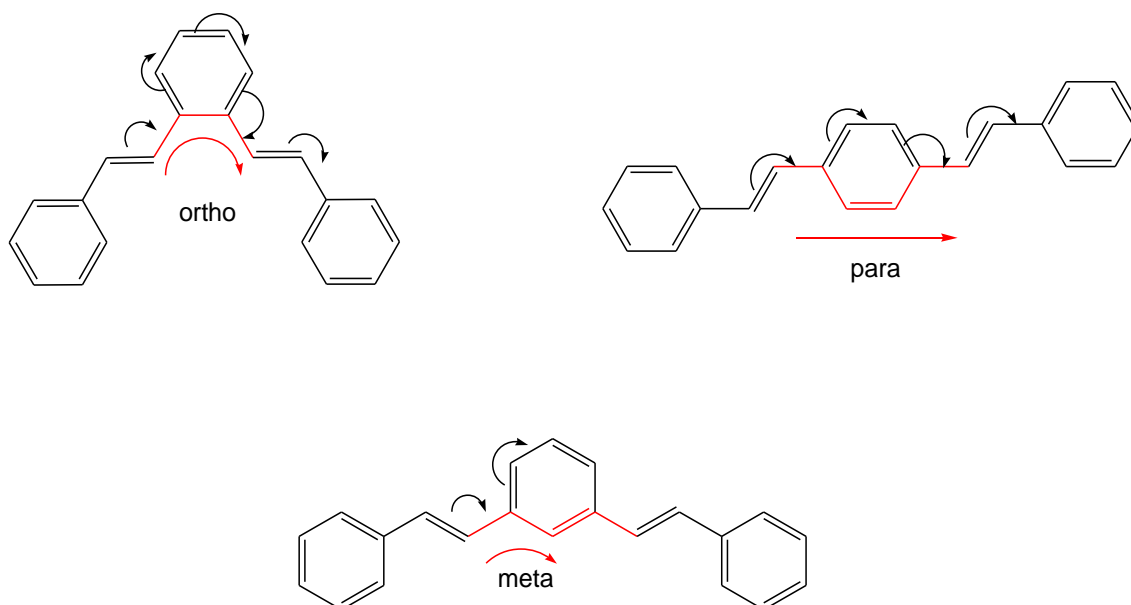


**Figure 13.** Illustrations of *ortho*-, *para*- and *meta*- conjugation paths

The efficiency of electron delocalization through an *ortho*-position phenyl bridge is as almost efficient as through *para*-position phenyl bridge if the  $\pi$ -conjugated backbone does not have large torsion angles and torsional motions (Huang *et al.*, 2011; Ali & Alvi, 2020). *Meta*-position phenyl bridge on the other hand, destroys the  $\pi$ -conjugation system in the molecule causing the localization of electron-hole pair as well as electronic decoupling which

affects the efficiency of facilitating the electron movement throughout the molecule (Teo *et al.*, 2017). As reported, *para*- position phenyl bridge dominates over *ortho*- and *meta*- positions ( $para > ortho > meta$ ). The difference between the strength of *para*- and *ortho*- positions might be because of the steric hindrance of *ortho*-substituents or chains which is then decrease the conjugation effects of the molecule (Ruiz-Carretero *et al.*, 2014; Serafini *et al.*, 2021).

According to the efficiencies results, compound **1c** shows higher efficiencies than compound **2c** by almost double of its amount. According to its structure, compound **1c** contains aromatic  $\pi$ -spacer with *para*- position meanwhile compound **2c** contains aromatic  $\pi$ -spacer with *ortho*- position. Thus, this confirms that the strength of the  $\pi$ -conjugation system in a molecule plays a role and can affect the efficiencies of DSSC device.

Therefore, based on the overall PCE results, compounds that contain aromatic  $\pi$ -spacers showed a higher conjugation effect compared to aliphatic  $\pi$ -spacers. This is because the  $\pi$ -electron delocalization was broken at the *ortho*-position in central phenyl ring. In other words, the *para*- position  $\pi$ -spacers can facilitate electron delocalization along molecule effectively. In addition, substituents also affected the overall efficiencies in terms of their electron donating effects where -OMe substituent showed the best results compared to -OH substituent, then followed by compound without any substituent. Thus, compound **1c** contains aromatic  $\pi$ -spacers with *para*-OMe substituents which gave the highest conversion efficiency.

## CONCLUSION

A total of eleven symmetrical bis-Schiff base compounds have been synthesized, characterized, and applied as dye-sensitizer for DSSC. Their power conversion efficiency were measured. The molecule with -OMe substituents and aromatic rings in *para*- position as the  $\pi$ -spacer bridge recorded the highest PCE overall. The presence of a conjugation system in the molecule as well as -OMe substituent as the electron donor allows sufficient electron delocalization along the molecule resulting in effective charge transfer within the molecule which is then transported to the TiO<sub>2</sub> layer on the working electrode. Conversely, boron difluoride Schiff base compounds recorded the lowest PCE in DSSC. The poor solubility in solvent system of both boron difluoride compounds may be the reason causing the low efficiency.

## ACKNOWLEDGEMENTS

The authors would like to thank Malaysian Ministry of Higher Education for the financial support to the research through Exploratory

Research Grant Scheme [ERGS/STG01(01)/1021/2013(01)]. In addition, NAH also would like to thank Universiti Malaysia Sarawak for providing scholarships and facilities for her Master study.

## REFERENCES

- Alattar, R.A., Hassan, Z.M., Abass, S.K. & Ahmad, L.M. (2020). Synthesis, characterization and study the photodecolorization of Schiff base Fe (III) complex in ZnO/Uv-A light system. In *AIP Conference Proceedings* (Vol. 2290, No. 1, p. 030032). AIP Publishing LLC.
- Alhamed, M., Issa, A.S. & Doubal, A.W. (2012). Studying of natural dyes properties as photosensitizer for dye sensitized solar cells (DSSC). *Journal of Electron Devices*, 16(11): 1370-1383.
- Alhorani, S., Kumar, S., Genwa, M. & Meena, P.L. (2021). Dye extracted from Bael leaves as a photosensitizer in dye sensitized solar cell. *Materials Research Express*, 8(11): 115507.
- Ali, R. & Alvi, S. (2020). The story of  $\pi$ -conjugated isotruxene and its congeners: From syntheses to applications. *Tetrahedron*, 76(35): 131345.
- Chouk, R., Aguir, C., Haouanoh, D., Bergaoui, M., Tala-Ighil, R., Stathatos, E. & Khalfaoui, M. (2019). A first-principles computational and experimental investigation on Schiff base cobalt complex towards designing solar cells. *Journal of Molecular Structure*, 1196: 676-684.
- Gul, M., Kotak, Y. & Muneer, T. (2016). Review on recent trend of solar photovoltaic technology. *Energy Exploration & Exploitation*, 34(4): 485-526.
- Houjou, H., Yagi, K., Yoshikawa, I., Mutai, T., & Araki, K. (2017). Effects of interaction between the chelate rings and  $\pi$ -conjugated systems in fused salphen complexes on UV-Vis-NIR spectra. *Journal of Physical Organic Chemistry*, 30(6): e3635.
- Huang, H.H., Prabhakar, C., Tang, K.C., Chou, P.T., Huang, G.J. & Yang, J.S. (2011). Ortho-branched ladder-type oligophenylenes with two-dimensionally  $\pi$ -conjugated electronic properties. *Journal of the American Chemical Society*, 133(20): 8028-8039.
- Ladomenou, K., Kitsopoulos, T.N., Sharma, G.D. & Coutsolelos, A.G. (2014). The importance of various anchoring groups attached on porphyrins

- as potential dyes for DSSC applications. *RSC Advances*, 4(41): 21379-21404.
- Lokhande, P.K.M., Sonigara, K.K., Jadhav, M.M., Patil, D.S., Soni, S.S. & Sekar, N. (2019). Multi-dentate carbazole based Schiff base dyes with chlorovinylene group in spacer for dye-sensitized solar cells: a combined theoretical and experimental study. *Chemistry Select*, 4(14): 4044-4056.
- Mahadevi, P. & Sumathi, S. (2020). Mini review on the performance of Schiff base and their metal complexes as photosensitizers in dye-sensitized solar cells. *Synthetic Communications*, 50(15): 2237-2249.
- Michael, P.R., Johnston, D.E. & Moreno, W. (2020). A conversion guide: solar irradiance and lux illuminance. *Journal of Measurements in Engineering*, 8(4): 153-166.
- Milichko, V.A., Shalin, A.S., Mukhin, I.S., Kovrov, A.E., Krasilin, A.A., Vinogradov, A.V., Belov, P.A. & Simovski, C.R. (2016). Solar photovoltaics: current state and trends. *Physics-Uspkhi*, 59(8): 727.
- Nain, P. & Kumar, A. (2021). Theoretical evaluation of metal release potential of emerging third generation solar photovoltaics. *Solar Energy Materials and Solar Cells*, 227: 111120.
- Pandey, A.K., Tyagi, V.V., Jeyraj, A., Selvaraj, L., Rahim, N.A. & Tyagi, S.K. (2016). Recent advances in solar photovoltaic systems for emerging trends and advanced applications. *Renewable and Sustainable Energy Reviews*, 53: 859-884.
- Pavia, D., Lampman, G. & Kriz, G. (2001). *Introduction to spectroscopy (3rd ed.)*. New York, USA: Saunders College Division.
- Phan, T.P., Teo, K.Y., Liu, Z.Q., Tsai, J.K. & Tay, M. G. (2019). Application of unsymmetrical bis-chalcone compounds in dye sensitized solar cell. *Chemical Data Collections*, 22: 100256.
- Ruiz-Carretero, A., Noguez, O., Herrera, T., Ramírez, J.R., Sánchez-Migallón, A. & de La Hoz, A. (2014). Microwave-assisted selective synthesis of mono- and bistriazines with  $\pi$ -conjugated spacers and study of the optoelectronic properties. *The Journal of Organic Chemistry*, 79(11): 4909-4919.
- Serafini, P., Milani, A., Tommasini, M., Bottani, C. E. & Casari, C.S. (2021). Topology-dependent conjugation effects in graphdiyne molecular fragments. *Carbon*, 180: 265-273.
- Shubbak, M.H. (2019). Advances in solar photovoltaics: Technology review and patent trends. *Renewable and Sustainable Energy Reviews*, 115: 109383.
- Tai, C.K., Chen, Y.J., Chang, H.W., Yeh, P.L. & Wang, B.C. (2011). DFT and TD-DFT investigations of metal-free dye sensitizers for solar cells: Effects of electron donors and  $\pi$ -conjugated linker. *Computational and Theoretical Chemistry*, 971(1-3): 42-50.
- Tay, M.G., Ngaini, Z., Arif, M.A.M., Sarih, N.M., Khairul, W.M., Lau, S.P.L. & Enggie, E. (2013). Complexation of bis-2-(benzylideneamino) phenol to cobalt(II) and zinc(II), and their spectroscopic studies. *Borneo Journal of Resource Science and Technology*, 3(1), 26-34.
- Teo, K.Y., Tiong, M.H., Wee, H.Y., Jasin, N., Liu, Z.Q., Shiu, M.Y., Tang, J.Y., Tsai, J.K., Rahamathullah, R., Khairul, W.M. & Tay, M.G. (2017). The influence of the push-pull effect and a  $\pi$ -conjugated system in conversion efficiency of bis-chalcone compounds in a dye sensitized solar cell. *Journal of Molecular Structure*, 1143: 42-48.
- Wang, M., Zhu, H., Jin, K., Dai, D. & Sun, L. (2003). Ethylene oligomerization by salen-type zirconium complexes to low-carbon linear  $\alpha$ -olefins. *Journal of Catalysis*, 220(2): 392-398.